Изв.вузов «ПНД», т.3, № 1, 1995 УДК 539.21

ANALYSING AND CONTROLLING CHAOS IN SPIN-WAVE INSTABILITIES

H. Benner, R. Henn, F. Rödelsperger, G. Wiese

Ferromagnetic samples excited by strong microwave fields show a variety of nonlinear phenomena. We report on magnetic resonance experiments in yttrium iron garnet (YIG) probing spin-wave instabilities above the first-order Suhl threshold. A variety of different scenarios, e.g. period doubling routes, quasiperiodicity, different types of intermittency together with a very complex multistability have been found and analysed. In the case of nonresonant excitation of the uniform mode the observed chaotic autooscillations correspond to a low-dimensional attractor ($D_2 \approx 2.1$) with a characteristic time scale of μs, whereas for resonant excitation very high-dimensional attractors ($D_2 \approx 7... >15$) are obtained. In order to stabilise unstable periodic orbits in such a fast system we developed an analog feedback device, which is related to the controlling scheme of Ott, Grebogi and Yorke. We succeeded in suppressing the low-dimensional chaos by applying a very small time-dependent feedback signal of about 10^{-3} the amplitude of the input microwave field.

1. Introduction

Magnetic insulators are very interesting objects for studying nonlinear dynamics, since even their simplest equation of motion

$$\dot{\mathbf{M}}(\mathbf{r},t) = -\gamma \mathbf{M}(\mathbf{r},t) \times \mathbf{H}_{\text{eff}}(\mathbf{r},t) + \text{dissipation} \qquad (1a)$$

contains intrinsically nonlinear terms. Considering non-fluctuating terms only and neglecting dissipation for a moment, the time evolution of magnetization is described by the torque of an effective field

$$\mathbf{H}_{\text{eff}}(\mathbf{r},t) = \mathbf{H} + \mathbf{h}\cos\omega t + A\mathbf{M}(\mathbf{r},t) + D\nabla^2\mathbf{M}(\mathbf{r},t) + \nabla\{\nabla\int d^3r' \, \mathbf{M}(\mathbf{r}',t)/|\mathbf{r} - \mathbf{r}'|\}, \qquad (1b)$$

where A - matrix.

For the systems of interest $\mathbf{H}_{\text{eff}}$ is composed of the external dc and ac magnetic fields, of demagnetizing and single-site anisotropy fields, of an exchange field, and of a dipolar field, depending themselves on the magnetization and giving rise to nonlinearities. Usually, this equation is discussed only for weak excitation ($h<<H,AM$,etc.) by linearizing its r.h. side with respect to deviations of $\mathbf{M}(\mathbf{r},t)$ from thermal equilibrium $\mathbf{M}_0$. However, even if confining ourselves to uniform magnetization, the exact solution of (1) shows a bistability (*«foldover effect»*) at moderate excitation amplitudes [1]. Moreover, the additional effect of the non-local exchange and dipolar fields may result in more complicated threshold phenomena indicating self-induced formation of spatio-temporal structures.

Part of these phenomena are well known for several decades from high-power ferromagetic resonance (FMR) experiments [2-5], and have theoretically been explained by Suhl [6] to result from the parametric excitation of spin waves through transverse pumping of the uniform mode. Suhl considered two cases, where the excitation of spin waves should be most efficient: *The first-order Suhl instability* results from the excitation of spin waves at half the pumping frequency, $\omega_k = \omega/2$, the second-order instability from spin waves at $\omega_k = \omega$. The specific properties of these instabilities have extensively been studied since a long time and have been reviewed in several articles [1,7-9].

During the last decade the progress of nonlinear dynamics has stimulated the reexamination of high-power FMR experiments under the more general aspect of deterministic chaos. Experiments, mostly performed on the low-dissipative prototype of a ferromagnet, yttrium iron garnet (YIG), have exhibited a variety of nonlinear phenomena, e.g. low-frequency auto-oscillations, period doublings, quasiperiodicity, mode-locking, intermittency, and chaos [9-18]. The experiments were mainly discussed in terms of models considering only a minimum number (2 or 3) of coupled spin-wave modes [17-21]. More realistic descriptions have taken into account the full degenerate spin-wave manifold [22-24] or are based on the direct integration of the equation of motion for $\mathbf{M}(\mathbf{r},t)$ [25].

Here, in an exemplary way, we focus on recent experimental results obtained on YIG spheres at the first-order Suhl instability (Sect.2). Since the complexity of this system can be varied within a wide range by the proper choice of external parameters (e.g. pumping frequency and input power, magnetic field, orientation, and temperature), it could be used as a (nearly) ideal model system for probing general concepts of nonlinear dynamics which generally work quite well in computer systems or in tailored mechanical or electrical devices, but often fail in real systems, especially in solid state physics. Several new and interesting phenomena have been observed: the occurrence of auto-oscillations starting directly at the Suhl threshold, a very complex multistability accompanied by sequences of bifurcations, different types of intermittency, including a new type of chaos-chaos intermittency and crises. We try to classify the observed pre-chaotic behaviour, report on techniques how to characterize the chaotic state, and present analyses of our data (Sect.3). A theoretical interpretation of these phenomena, taking into account the specific properties of long-wave modes, has been developed by us in a series of papers [26-29], but is beyond the scope of this article.

Finally, we consider the topical problem concerning the possibility of chaos suppression by stabilizing inherent unstable periodic orbits with the help of very weak external perturbations. By means of an analogy feedback device related to the controlling scheme of Ott, Grebogi, and Yorke (OGY)[30] we succeeded in suppressing the observed chaotic signal by a small time-dependent perturbation of the applied microwave power (Sect.4). To our knowlege, this experiment represents the fastest system controlled so far by a feedback system which stabilizes the inherent periodic dynamics of a strange attractor.

2. Experiments in YIG Spheres

2.1. Subsidiary absorption and coincidence regime. The first-order Suhl instability is characterized by the decay of the externally driven uniform mode into two spin waves of half the pumping frequency $\omega_k = \omega_p/2$ and opposite wave vectors ($\mathbf{k}$, $-\mathbf{k}$) according to the conservation of energy and quasi-momentum. This instability can either be observed off resonance (i.e. with the pumping frequency ω_p far away from the usual ferromagnetic resonance ω_0) as a *subsidiary absorption*, or directly on resonance ($\omega_p=\omega_0$) within the *coincidence regime*. Profiting from the resonance amplification of the uniform mode, experiments in the coincidence require much less microwave power to reach the threshold (for pure YIG three orders of magnitude less).

For spherical samples the eigenfrequency of the uniform mode ω_0, which describes the uniform precession of the spins around the external magnetic field $\mathbf{H}\|z^\wedge$, is given by

$$\omega_0 = \gamma(H + H_a). \quad (1)$$

H_a describes the influence of weak cubic crystal field (cf. Table1) which depends on sample orientation and can generally be neglected. The uniform mode is driven by a transverse homogeneous microwave field $h\cos(\omega_p t)\hat{x}$ at a pumping frequency ω_p. The dispersion relation ω_k of plane spin waves with a wave vector **k** and a propagation angle $\theta_k = \angle(\mathbf{k}, \mathbf{H})$ reads [1]

$$\omega_k^2 = \gamma^2(H_i + Dk^2)(H_i + Dk^2 + 4\pi M_S \sin^2\theta_k), \quad (2)$$

where $\gamma = g\mu_B/\hbar$ denotes the gyromagnetic ratio, D the stiffness constant and M_S the saturation magnetization. The internal magnetic field $H_i \equiv H + H_a - 4\pi M_S/3$ includes the demagnetizing field of the sphere. The dependence on θ_k reflects the anisotropy of the dipolar interaction and gives rise to a band of spin waves, the lower edge corresponding to spin waves which propagate parallel to **H** and the upper edge to those which propagate in perpendicular direction.

The first-order instability only occurs if $\omega_p/2$ exceeds the bottom of the spin-wave band, which is the case for

$$\omega_p \geq 2\gamma H_i. \quad (3)$$

Normally this condition can only be fulfilled for off-resonance excitation of the uniform mode. In this case subsidiary absorption shows up in a field scan as a broad structure below the main FMR line, which was the standard situation in previous experiments. Only in low fields it is possible to observe the instability on resonance ($\omega_p = 2\omega_k = \omega_0$). The corresponding field range of this so-called *coincidence regime* is limited by [6]

$$4/3\pi\gamma M_S \leq \omega_p \leq 8/3\pi M_S. \quad (4)$$

The upper limit follows from (1) and (3), the lower limit from the vanishing of the FMR signal due to the formation of magnetic domains for $H_i < 0$. For pure YIG samples at room temperature this regime occurs for pumping frequencies $\omega_p/2\pi$ between 1.7 and 3.3 GHz, corresponding to external magnetic fields between about 700 and 1300 Oe for **H**|| (100).

In order to determine the critical modes which are the first to become unstable at the threshold one has to minimize the critical amplitude b_0 of the uniform mode for exciting a pair of eigenmodes at $\omega_k = \omega_p/2$. In the case of plane spin waves (**k**, **-k**) this critiical amplitude is given by [1]

$$|b_{0,\mathrm{crit.}}| = \eta_k/|\rho_{kk'}|, \quad |\rho_{kk'}| = 4\pi\gamma M_S \sin\theta_k \cos\theta_k \,(\omega_k + \gamma H_i + \gamma D k^2)\, \delta_{\mathbf{k},-\mathbf{k}}/\omega_k, \quad (5)$$

where η_k denotes the spin-wave damping and $\rho_{kk'}$ the dipolar coupling coefficient. Assuming the spin-wave damping η_k to be constant, the minimum threshold is obtained for $\theta_k = 45°$ as long as $\omega_p/2$ meets the 45°-branch of the spin-wave band. Then we have $k >> d^{-1}$ (inverse sample diameter), and the plane-wave approximation can be applied. If $\omega_p/2$ is below the 45°-branch, one expects the excitation of longwave modes with $k \to 0$ (Fig.1), which are not adequately described by the plane-wave approximation. Hence, the analysis of our data has to be based on a generalized type of eigenmodes including the boundary conditions of the sample as proposed by Wiese [28]. In practice, this means that (5) has to be adapted to this more appropriate type of eigenmodes. A detailed analysis of the critical modes, which is based on the experimental observation of a distinct fine structure occurring at the threshold, has been presented recently [28,29].

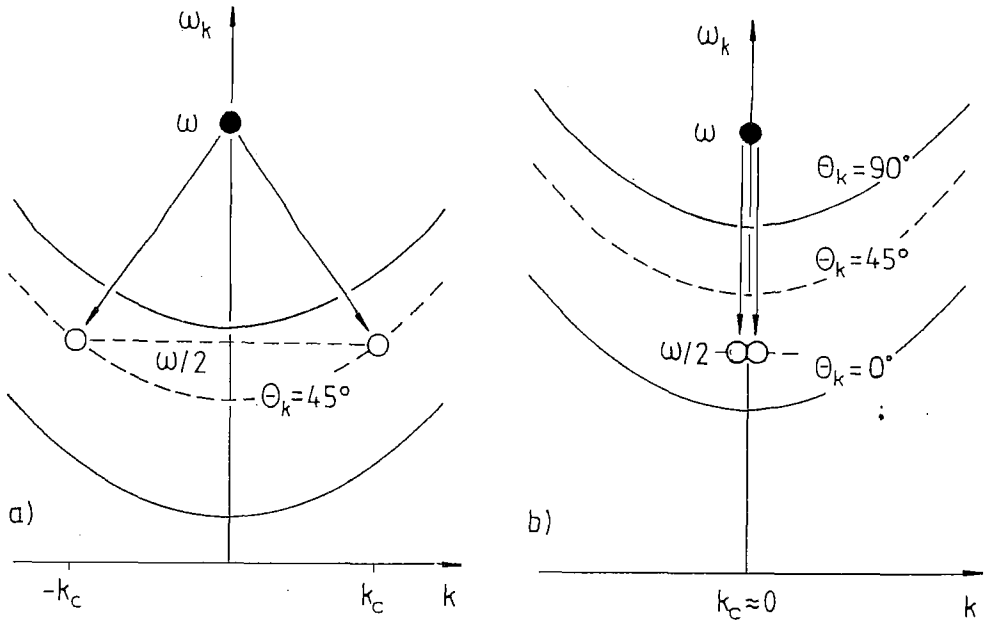

Fig. 1. Parametric excitation of non-uniform modes at the first-order Suhl instability ($\omega_k = \omega_p/2$). a) Excitation of spin waves ($k_c \approx 10^4$ - 10^5 cm^{-1} and $\theta_k \approx 45°$) in low magnetic field. b) Excitation of long-wavelength modes ($k_c \to 0$ and $\theta_k < 45°$) in higher magnetic field

Table. Properties of spherical YIG samples

	T =300 K	T =4.2 K
saturation magnetization $4\pi M_S$	1780 Oe	2440 Oe
gyromagnetic ratio $\gamma/2\pi$	2.798 MHzOe^{-1}	2.798 MHzOe^{-1}
stiffness constant D	4.48x10^{-9} Oe cm^2	4.24x10^{-9} Oe cm^2
anisotropy field H_a, H||<100>	+ 90 Oe	+ 260 Oe
H||<111>	- 50 Oe	-140 Oe
coincidence regime $\omega_p/2\pi$	1.66 - 3.32 GHz	2.28 - 4.56 GHz

2.2. Experimental Set-up. A prototype ferromagnet used most often for the investigation of nonlinear spin dynamics is yttrium iron garnet $Y_3Fe_5O_{12}$ [31]. Its important advantages are a rather strong magnetization even at room temperature and extremely narrow resonance lines of both the uniform mode ($\Delta H_0 \equiv 2\,\eta_0/\gamma < 1$ Oe) and of the spin waves ($\Delta H_k \equiv 2\eta_k/\gamma \approx 0.3$ Oe) resulting in a very low threshold for spin-wave instabilities. Note that the threshold amplitude in the coincidence regime only amounts to $h_{c1} \approx \Delta H_0 \Delta H_k / 8\pi M < 1$mOe, corresponding to an irradiated power of some 50 μW.

In view of such small thresholds, «high power» FMR experiments, in principle, can be performed with a conventional ESR spectrometer. We studied the subsidiary absorption, for example, at 9.3 GHz by means of a bimodal transmission type cavity of quality factor 3000. For our experiments in the coincidence regime we preferred a broad-band (1 - 4 GHz) transmission-type set-up (Fig.2). For the transverse excitation and detection of the uniform mode, instead of a microwave cavity, we used two microcoils with perpendicular orientation in order to minimize mutual disturbations by crosstalk. The squared amplitude of the driving field h at sample position was proportional to the input power P_{in} supplied by the microwave source. The signal transmitted to the pick-up coil was amplified and detected by a diode. Within the quadratic regime of the diode, the

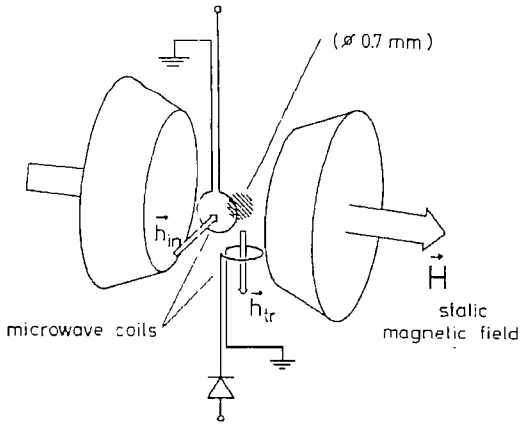

Fig. 2. Experimental set-up. The driving coil (1 - 4 GHz) is directly fed by a very stable microwave generator. The signal transmitted to the pick-up coil is amplified, rectified, and recorded by a digital oscilloscope

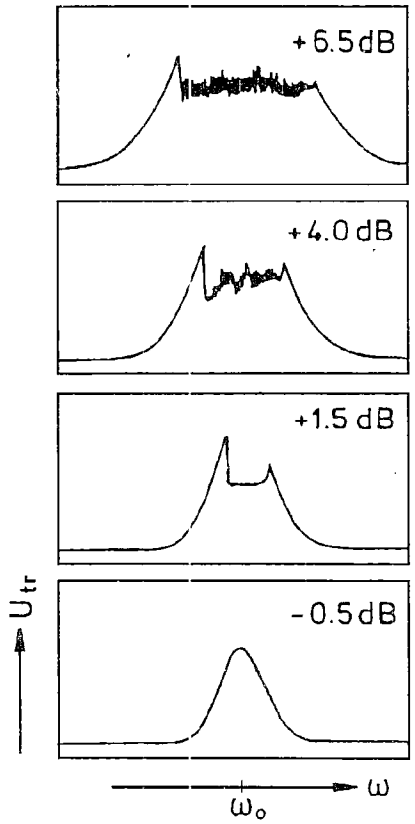

Fig. 3. Shape of the FMR line below and above the Suhl threshold (denoted by «0 dB»). Frequency scale: ± 10 MHz·2π. The asymmetric breaks show hysteresis effects and time-dependent oscillations

rectified signal was proportional to the squared amplitude $|b_0|^2$ of the uniform mode, i.e. to the transmitted power P_{tr}. By means of a digital oscilloscope and an integrating voltmeter we recorded both the time dependence of $P_{tr}(t)$ and its average value P_{tr} - with respect to the input power P_{in}.

The presented data were obtained at room temperature on a highly polished sphere of pure YIG with 0.71 mm diameter. We generally used the orientations **H**||(100),**H**||(111), or the «30° orientation», where the crystal is rotated by 31.7° from the (100) to the (111) direction. For the latter orientation H_a is exactly zero.

2.3. Observed Phenomena. While in conventional off-resonance FMR experiments ($\omega_p=2\omega_k\neq\omega_0$) the first-order Suhl threshold occurs as a broad «subsidiary» absorption structure in lower field [2], the threshold within the coincidence regime ($\omega_p=2\omega_k=\omega_0$) shows up even more pronounced as a sharp and asymmetric break at the top of the line. This break becomes broader with increasing input power and shows «noisy» oscillations (Fig.3). The coincidence condition means that ω_p and H are locked to resonance and only varied simultaneously.

The coincidence regime of the investigated YIG sphere was found to range from 1.8 to 3.4 GHz (680 - 1280 Oe for **H**|| (100)). Below 680 Oe the FMR signal vanishes due to the occurrence of magnetic domains. Above 1280 Oe a drastic increase of the threshold takes place, indicating the changeover from the first- to the second-order Suhl instability. The intermediate field range may be divided into three regimes (Fig.4) differing by their characteistic behaviours:

(i) *Regime* A (680-760 Oe): Up to the Suhl threshold P_{tr}- increases linearly with P_{in}, indicating that only the uniform mode is excited. Above the threshold P_{tr}- remains constant for a range of nearly 10 dB. No oscillations are observed, until finally a sudden jump of P_{tr}- occurs, accompanied by a transition from constant to chaotic time dependence of $P_{tr}(t)$ and by a weak hysteresis.

(ii) *Regime* B (760-1030 Oe) is characterized by a variety of sudden jumps of P_{tr}- starting directly above threshold, accompanied by the occurrence of a complicated multistability. If P_{in} is again decreased af-

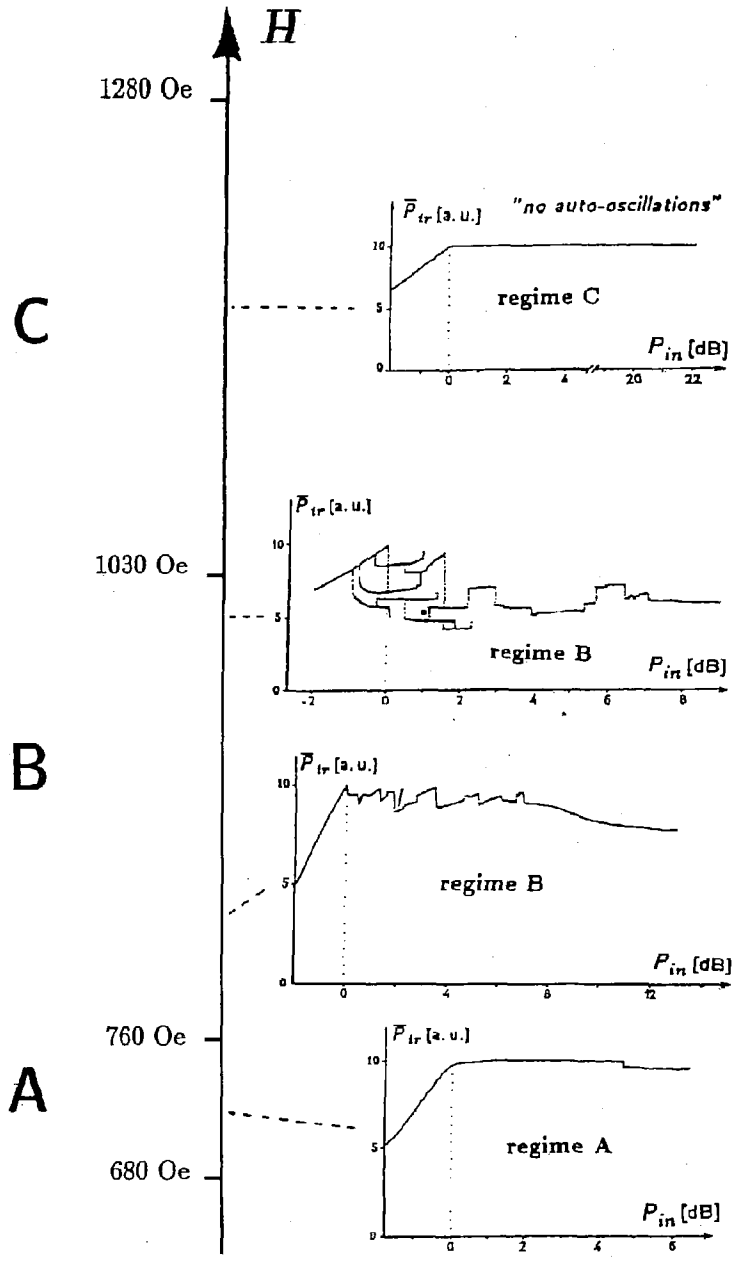

Fig. 4. Average transmitted FMR signal P_{tr} vs. input power P_{in} on variation of the magnetic field. Regime B is characterized by a variety of jumps and multistable behaviour which is connected with rather complex time dependences. A and C differ from B by their constant and time independent behaviour above threshold

ter a jump, the system remains on the new level. Variation of P_{in} yields a number of new levels, i.e. for the same input power there exist several stable states, sometimes up to ten. Simultaneously, the system shows very complex types of time dependence. We observed constant behaviour, periodic and quasiperiodic oscillations, intermittency and chaos. Generally, the oscillation amplitudes are less than 10% of P_{tr}, and frequencies occur between 10 and 600 kHz, most often between 30 and 200 kHz, apart from higher harmonics. The sudden jumps of P_{tr} are always accompanied by an abrupt change of the observed time dependence. As long as P_{tr} remains on the same level, $P_{tr}(t)$ shows only

continuous variations of the oscillations or bifurcations without any hysteresis (e.g. transitions from constant to periodic, from periodic to quasiperiodic, locking phenomena, period doublings). About 5 - 10 dB above threshold the system becomes chaotic, showing various kinds of irregularity at higher input power, e.g. multiple chaotic attractors, high-dimensional intermittency and crises. Moreover, the corresponding chaotic levels sometimes appear already at lower power within the regime of regular behaviour. The experiment turns out to be very sensitive to the control parameters ω and H; a detuning of H by only 0.2 Oe was already sufficient to change the level structure. Nevertheless, the levels could be reproduced even after several weeks.

(iii) *Regime* C (1030-1280 Oe): Qualitatively, the behaviour resembles very much that of regime A. P_{tr} remains constant above the threshold, and oscillations occur only at higher excitation. The transition to chaos also occurs at higher input power (20 - 30 dB above the Suhl threshold).

For other sample orientations (**H** parallel to the (110) or (111) directions) we found very similar behaviour, but the three regimes were shifted in field (by - 100 Oe and - 140 Oe, respectively).

We interpret these different regimes to be related to the different types of parametrically excited modes. It is obvious to identify A with the regime of spin waves with $k \approx 10^4$-10^5 cm^{-1} and $\theta_k \approx 45°$, whereas in B and C Suhl's theory predicts the excitation of long-wavelenght modes ($k \to 0$). Apparently, the observed discontinuities in B are related to the discreteness of these modes. The different behaviour of C, however, cannot be understood in terms of the conventional theory, but requires a more detailed discussion [26,29].

2.4. Scenarios. Experimentally, one cannot exclude a very fine-graduated locking to rational frequency ratios similar to a devil's staircase, but this would be rather unlikely.

Under the aspect of nonlinear dynamics the most interesting phenomena were observed at coincidence in regime B. To get a more systematic impression of the observed oscillations, a large number of time series of $P_{tr}(t)$ - up to 16000 data points each - was recorded on variation of P_{in} or some other control parameter. The corresponding power spectra were obtained by Fourier transformation, and their strongest spectral components were plotted versus the parameter under variation. This way, one obtains a number of «maps» visualizing the dependence of the oscillation frequencies on various control parameters. Such maps are useful for classifying the observed routes to chaos.

As a general result, we found that a global correspondence to one of the well-known scenarios of *Feigenbaum, Ruelle-Takens-Newhouse* or *Pomeau-Manneville* [32] does not occur, but a variety of parts from all of them. This obviously corresponds to the fact that the nonlinearities of our real system are more complicated and based on a larger number of internal degrees of freedom than represented by the simple maps where these standard routes have been derived from. The physical meaning of these degrees of freedom is probably that of specific eigenmodes or a collective motion of several of them. Thus, a jump from one level to the other might correspond to a sudden change of the number of degrees of freedom induced by the coupling or decoupling of certain modes.

Often quasiperiodicity was observed with up to three fundamental frequencies. A typical example, suggesting an interpretation in terms of the Ruelle-Takens scenario, is shown in Fig.5. Very close above threshold (denoted by «0 dB») the system starts oscillating at about 130 kHz, that means, a first Hopf bifurcation changes the *fixed point* into a *limit cycle*. At 2.5 dB a second fundamental frequency of 40 kHz occurs - corresponding to a second Hopf bifurcation - together with several sum and difference frequencies of harmonics. Note that no jump is observed in P_{tr}. With increasing microwave power both oscillation frequencies seem to vary independently[1], indicating that the attractor is a *2-torus*. This quasiperiodic oscillation remains stable for about 1dB. Then, according to Ruelle and Takens, one would expect a third Hopf bifurcation and the immediate break of the arising unstable *3-torus* to chaos. The different behaviour observed

[1] Experimentally, one cannot exclude a very fine-graduated locking to rational frequency ratios similar to a *devil's staircase*, but this would be rather unlikely.

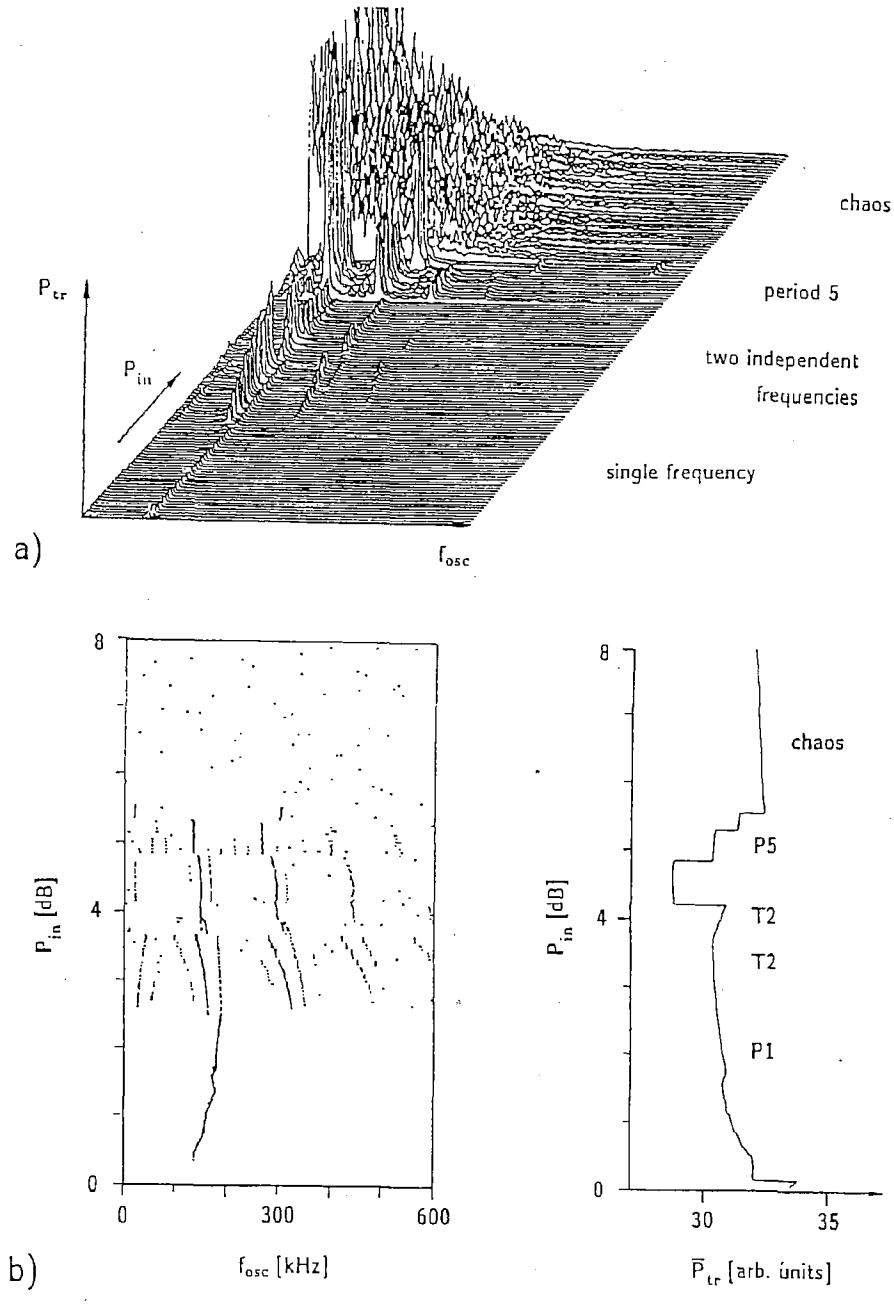

Fig. 5. Power spectra of auto-oscillations in Regime B with respect to P_{in} (input power is scaled to the Suhl threshold). a) Three-dimensional «landscape» of spectral components. b) «Map» of oscillation frequencies; the corresponding level of $\overline{P}_{tr}$ is presented in the r.h.s. diagram. The system shows quasiperiodic behaviour and mode-locking

in our experiment can be interpreted by the spin system switching over to a coexisting stable attractor. Nevertheless, we also found experimental examples where a third fundamental frequency occurred for an extended parameter range. There are other levels where the different frequencies tend to lock. At 5 dB, for instance, instead of quasiperiodicity a period-5 (P5) oscillation takes place. Low-period oscillations, such as P2, P3, P4 or P6 were observed rather often, but sometimes also higher periods of 11 or even 25. The changeover to chaos is generally accompanied by a jump of $\overline{P}_{tr}$. Since in most cases this

changeover does not start from a 2-torus, it cannot be related to the third bifurcation of a Ruelle-Takens scenario. We rather suppose that the chaotic behaviour results from a sudden increase of the number of coupled modes, which is related to some global symmetry-breaking bifurcation [33], and does not follow one of the standard routes.

A period-doubling route, as reported previously from both transverse and parallel pumping experiments [10,12], was observed up to period 8 but occurred rather seldom. More often, only a single period doubling occurred, remaining stable for an extended range of P_{in} and then changing directly over to chaos. Though the Feigenbaum route is known to be very sensitive to noise which might suppress the subsequent period doublings, we rather interpret the observed behaviour to present an independent route. We also observed a sequence of period triplings (not to confuse with a period-3 window!) up to period 9.

By intermittency we mean the occurrence of a signal which randomly alternates between two (or more) different types of time behaviour, e.g. laminar phases and irregular bursts (Fig.6). Three universal types of intermittency (I - III) have been derived by Pomeau and Manneville [34] corresponding to the basically different ways how a fixed point of a 1D map can lose its stability. Often these types can already be distinguished from their characteristic time behaviour, but also from a reconstruction of the generating map and from the distribution and scaling behaviour of the laminar lengths [32]. Intermittency, so far, has been found rather seldom in magnetic systems, and only the observation of the Pomeau - Manneville type III has been reported in literature [35]. Both in the coincidence regime and for subsidiary absorption we observed various kinds of intermittency starting from a fixed point, a limit cycle, a 2-torus, or even alternating between different chaotic states (Fig.6e,f). From analyzing the distribution and scaling

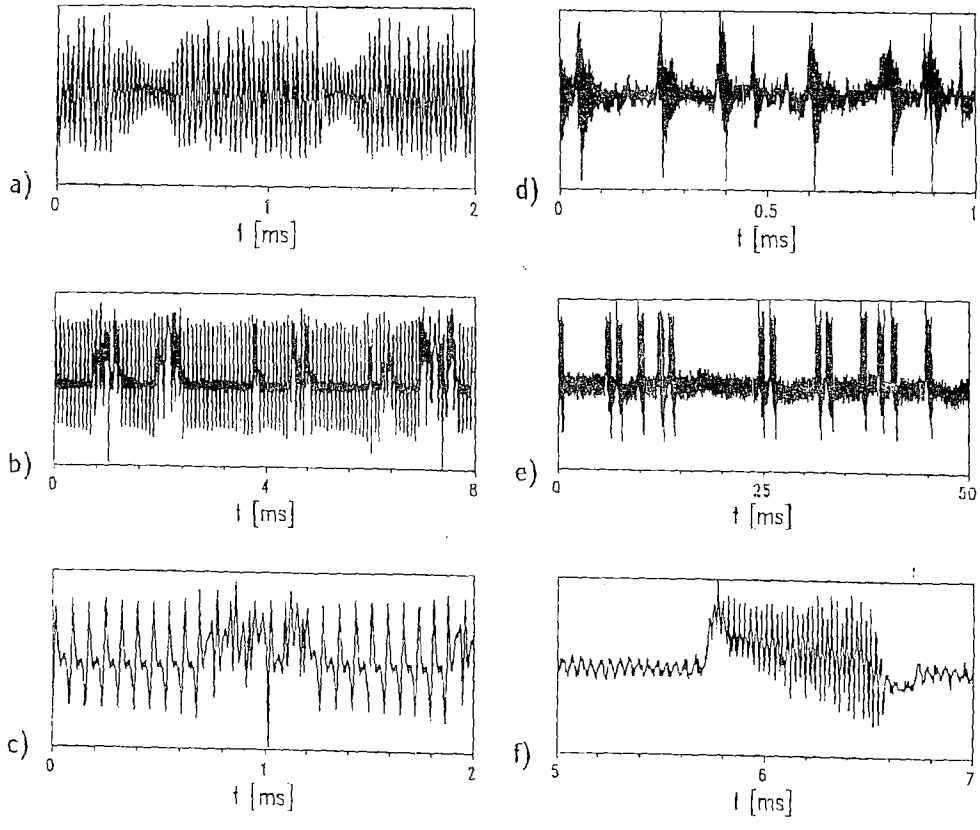

Fig. 6. Different types of intermittency, observed in the coincidence regime (a-c, e, f) and in subsidiary absorption(d). a) Pomeau-Manneville type I , b) type III , c) extended time scale of b). d) Homoclinic crisis. e) Chaos-chaos intermittency due to a global symmetry-braking bifurcation, f) extended time scale of e)

behaviour of the 'laminar' lengths, the observed signals could clearly be attributed to each of the universal types I, II or III or to crises [33,36]. It is interesting to note that the Pomeau - Manneville types are generally observed in parameter regimes where the system remains *low-dimensional* (see next section), whereas chaos-chaos intermittency occurs at *higher dimension*, especially in the coincidence regime. We found that in most cases chaos-chaos intermittency scaled like the Pomeau - Manneville type III [36] which is not consistent with the common interpretation of arising from a crisis [37]. Very recently this specific behaviour was interpreted in terms of a global symmetry-breaking bifurcation which seems to be related to the excitation of an additional spin-wave mode [33].

For the coincidence regime it is impossible, because of the very complex multistability, to present a global diagram showing the dependence of these various scenarios on e.g. magnetic field and microwave input power. For subsidiary absorption, we have systematically analysed the dynamic behaviour of the parametric excitation signal observed at room temperature at a fixed pumping frequency of 9.26 GHz. Typical scenarios and the respective bifurcation lines in a two dimensional control parameter space, spanned by the magnetic field H and the applied microwave power P_{in}, are represented in Fig.7. The lower line shows the dependence of the Suhl threshold (the so-called *butterfly curve*) on H. The broad bumps at 1.6 and 1.9 kOe have been attributed to the excitation of discrete magnetostatic modes [38]. The steep increase of the threshold at 2.2 kOe corresponds to the fact that $\omega_p/2$ falls below the spin-wave band. The bifurcation line above indicates the onset of autooscillations. The local scenarios occuring at higher P_{in} show similarities with the behaviour observed at the coincidence regime: again we have three regimes with essentially different behaviours. Especially in B we have areas of period doublings, quasiperiodicity, intermittency, and chaos in very close vicinity, and the observed behaviour depends very much on the chosen variation of parameters. We observed several codimension-2 bifurcations, e.g. at 1650 Oe/11dB where a supercritical Hopf bifurcation meets a subcritical one, giving rise to intermittency of Pomeau - Manneville type II. Intermittency of type III was observed at 1990 Oe/10 dB characterizing the tran-

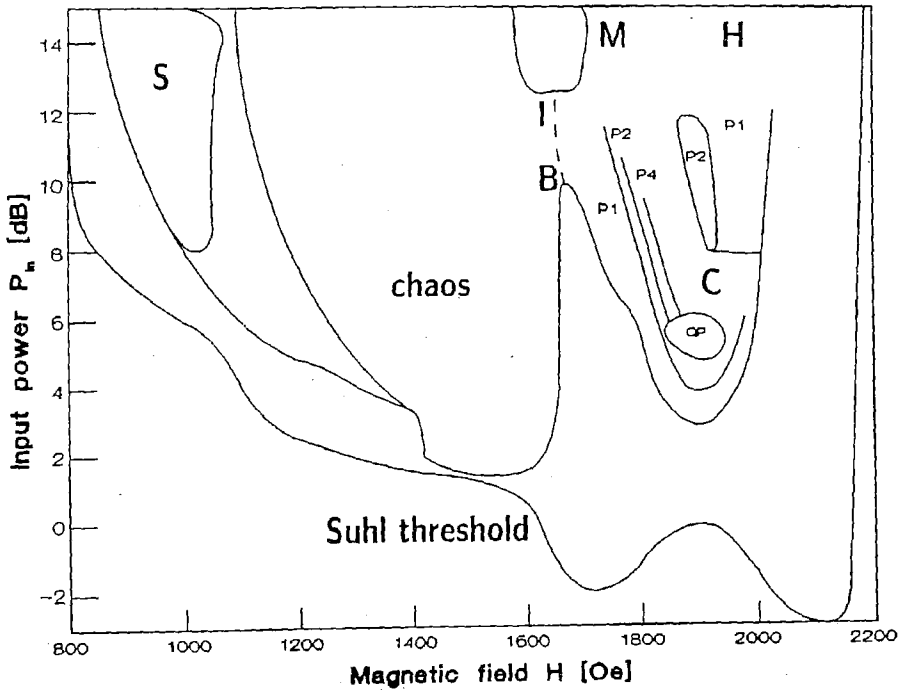

Fig.7. Codimension-2 scenario in subsidiary absorption. The lower line indicates the Suhl threshold, the next upper line the onset of autooscillations. **M**: multistability, **H**: homoclinic crisis, **S**: small amplitude crises, **I**: intermittency of Pomeau - Manneville type II, **B**: codimension-2 bifurcation, **P1- P4**: period doubling bifurcations, **QP**: quasiperiodic behaviour, C: marginal chaos, application of OGY control

sition from a period-2 oscillation into chaos. At higher power we also observed both homoclinic crises and multistability, which in subsidiary absorption plays only a minor role.

3. Characterization of chaos from experimental data

The chaotic behaviour of a dissipative system can be attributed to the existence of a *strange attractor* describing its asymptotic long-time behaviour (without transients) in phase space. The property which makes the attractor strange is its sensitive dependence on the initial conditions: despite the contraction in phase space volume, lengths need not simultaneously shrink in *all* directions, and points, which are infinitesimally close at the beginning, become exponentially separated for sufficiently long times. Specific techniques have been developed to determine the characteristic properties of a strange attractor, e.g. its topological structure or the time scales of exponential separation. For details see e.g. the textbooks by Schuster [32] or Bergé et al. [39].

3.1. Lyapunov exponents, entropies, dimensions. In order to quantify specific properties of strange attractors - e.g. its topological structure or the strength of chaos - a special notation has been developed and appropriate methods to probe them.

The distortion of a d-dimensional volume element in phase space is characterized by a set of *Lyapunov exponents* λ_i , $i=1, \ldots, d$, describing the evolution of distances δx_i along the local eigendirections of distortion at a given point $\mathbf{x}(t_0)$:

$$\delta x_i (t) = e^{\lambda i (t - t_0)} \delta x_i(t_0). \tag{6}$$

Necessary and sufficient for the occurrence of chaos is the condition that at least one of these exponents has to be positive, giving rise to the exponential divergence of neighbouring trajectories.

The *Kolmogorov entropy* K is the sum of all positive Lyapunov exponents averaged over the whole attractor [40] and, thus, a measure how fast information on the present state of motion gets lost. Its reciprocal value gives the time scale where the behaviour of a chaotic system is still predictable. For example, a regular system (no positive Lyapunov exponent!), which can be predicted for infinite times, has the entropy $K=0$. Noise, as a purely stochastic and unpredictable process, is characterized by $K \to \infty$. Chaotic behaviour is somewhere in between, and, again, $K>0$ is a necessary and sufficient criterion for the occurrence of deterministic chaos.

Another interesting quantitative characterization of chaotic behaviour is given by a set of *generalized fractal dimensions* D_q characterizing the topological structure of the attractor:

$$D_q = \lim_{\varepsilon \to 0} \frac{1}{q\text{-}1} \log \left(\sum_{i=0}^{M(\varepsilon)} p_i^q \right) / \log \varepsilon \, , \tag{7}$$

q is an integer classification index, $M(\varepsilon)$ is the number of phase space cells of size ε visited by the attractor and p_i is the probability to visit the i-th cell. The D_q are generalizations of the usual Euclidean dimensions allowing the characterization of self-similar geometrical objects. The D_q differ by the weight of the local probabilities which is interesting for inhomogeneous attractors. D_0 is the well-known *Hausdorff - Besicovich dimension*, D_1 is called the *information dimension* and D_2 the *correlation dimension*.

All strange attractors investigated so far show fractal, i.e. noninteger, dimensions, so the fractal property is considered as an additional signature of chaos. The physical importance of analyzing the dimension is to get some idea of the minimum number of degrees of freedom necessary for modelling the system.

3.2. Reconstruction of the phase space. One of the basic problems when analyzing experimental data concerns the reconstruction of the underlying chaotic attractor from a time series of experimental data representing only a single component $U(t)$. Every reconstruction of phase space is based on the implicit assumption that each observable

reflects sufficiently well the overall behaviour of the system to permit a complete analysis. Different methods can be used to define the vectors of the reconstructed space:

(i) The components of a d-dimensional vector $\mathbf{x}(t)$ of the new phase space are built up by the signal $U(t)$ successively shifted in time by a certain delay τ:

$$\mathbf{x}(t) = \{U(t), U(t+\tau), \ldots, U(t+(d-1)\tau)\}. \tag{8}$$

Because of its simplicity this *method of time delay coordinates* [41] is widely used for the analysis of both experimental data and numerical simulations.

(ii) Instead of using delayed coordinates we can also treat $U(t)$ and its time derivatives as independent components of a substitute vector

$$\mathbf{x}(t) = \{U(t), \dot{U}(t), \ddot{U}(t), \ldots U^{(d-1)}(t)\}. \tag{9}$$

For data acquisition, generally the second method is more laborious to apply, but it can be of advantage, when the derivative signals are obtained by an analog technique.

The reconstruction does not yield an attractor identical with that in the original phase space, but merely retains general topological properties, which may be sufficient for studying its essentials, such as dimensions, exponents or entropies.

3.3. Analysis of time series data. Following the work of Grassberger and Procaccia [42] we confine ourselves to estimates of D_2 and K_2.

As an example, we present the analysis of correlation dimension and entropy by means of the well-known method of Grassberger and Procaccia [42], applied to the chaotic signals of our experiment.

In a first step, we reconstruct the new phase space vectors $\mathbf{x}_i \equiv \mathbf{x}(t_i)$ of the attractor by means of the time delay method, as described in the preceding section.

In a second step, from N of such vectors $\mathbf{x}_i$ the *correlation integral*[2]

$$C_d(l) = \lim_{N\to\infty} \frac{1}{M} \sum_{i=1}^{M} \frac{1}{N} \sum_{j=1}^{N} \Theta[l - ||\mathbf{x}_i - \mathbf{x}_j||] \tag{10}$$

is calculated, where N denotes the total number of data points, M the number of reference points, $\Theta(x)$ the Heaviside function, l a distance parameter and $||\mathbf{x}||$ some arbitrary norm, e.g. Euclidian norm. The correlation integral $C_d(l)$ counts the number of pairs of d-dimensional vectors with a distance $||\mathbf{x}_i - \mathbf{x}_j||$ smaller than a given value l. Grassberger and Procaccia [36] have shown that for sufficiently large embedding dimensions the correlation integral scales like lD_2 and, therefore, can be used to estimate the correlation dimension:

$$D_2 \approx \lim_{l\to 0} \lim_{d\to\infty} \frac{\log C_d(l)}{\log l}. \tag{11}$$

To this end, $\log C_d(l)$ is plotted vs. $\log l$ (Fig.8). In practice, since the limit $l\to 0$ cannot be reached, the slope of the curve is taken instead. The limit $d\to\infty$ is not essential and is taken only to guarantee a proper embedding. In addition, the correlation entropy K_2 can be obtained from the vertical distance of two neighbouring curves $\log C_d(l)$ and $\log C_{d+1}(l)$ at fixed l [42]:

$$K_2 \approx -\lim_{\tau\to 0} \lim_{l\to 0} \lim_{d\to\infty} 1/\tau(\log C_{d+1}^2(l) - \log C_d^2(l)). \tag{12}$$

Here, the limit $d\to\infty$ results from the original definition of K_2 [32] and is necessary to obtain the correct asymptotic behaviour.

In order to get some idea of the minimum number of relevant degrees of freedom involved in the evolution, we have systematically analysed the correlation dimension of our data. To this end we have evaluated a large number of time series of $P_{tr}(t)$, up to

---

[2] Following the work of Grassberger and Procaccia [42] we confine ourselves to estimates of D_2 and K_2.

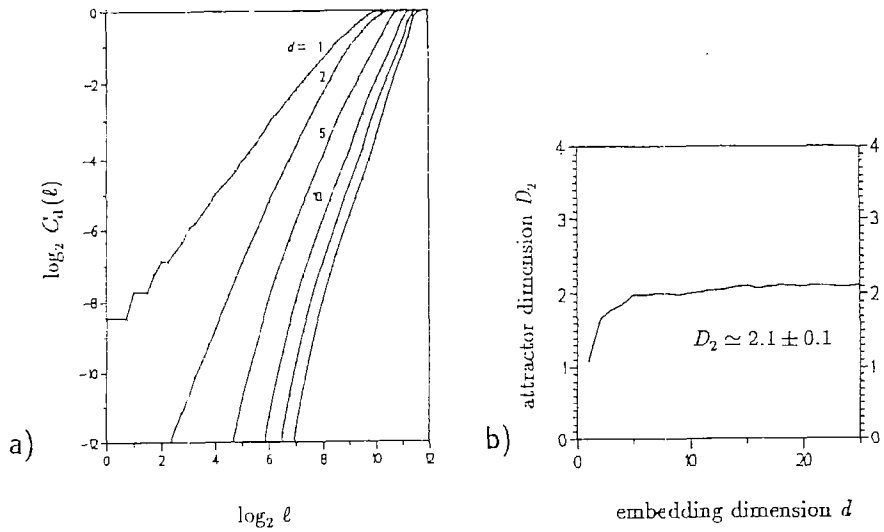

Fig. 8. Grassberger - Procaccia analysis of a chaotic signal. a) Log-log plot of the correlation function vs. distance parameter l. b) Attractor dimension D_2 as a function of the embedding dimension. The chaotic signal investigated was observed in subsidiary absorption at $\omega/2\pi$=9.26 GHz, H=1.83 kOe and P_{in} =7.5 dB (see Fig.7)

16000 points each, taken from the whole investigated parameter range. For regular signals we found values of D_2 close to 1 or 2, in some cases even close to 3, as expected from the power spectra. A typical signal observed at subsidiary absorption is presented in Fig.8. Our analysis yields a correlation dimension of 2.1±0.1, indicating very weak («*marginal*») chaos, and a correlation entropy of about $0.04(\mu s)^{-1}$.

In the coincidence regime chaotic signals, in general, showed higher dimensions ranging from 5 to larger than 15. We already mentioned that multistability also occurs in the chaotic regime, indicating the coexistence of several strange attractors (Fig.9). At 10 dB e.g. there occur two separate levels of chaotic oscillations differing markedly in amplitude, but also in fractal dimension. We even observed a different tendency of variation with respect to the control parameter; while on the lower level D_2 was found to increase with P_{in}, it was decreasing on the upper one.

In total, this analysis supports our earlier impression that jumps of P_{tr}- are related to discontinuous changes of relevant degrees of freedom. As long as the system remains on the same level, only slight and continuous changes of D_2 occur on variation of P_{in} , whereas D_2 changes drastically at every jump. It is obvious to ascribe such behaviour to some nonlinear mechanism «switching certain modes on or off» with respect to the control parameters and to the previous state of the system. This idea is supported by the model developed by Wiese [26-28], which is based on a novel indirect coupling via degenerate magnetostatic modes.

4. Controlling chaos

This choice of coordinates, in addition, avoids a possible instability of the controlling algorithm which may occur in the case of time-delay coordinates [47]. A general problem of current interest concerns the possibility of *controlling* the chaotic behaviour of nonlinear systems, which means to change the irregular into a regular behaviour, without drastically affecting the system parameters. The practical use of such a control would be to suppress undesired irregularity and to select among a large number of possible regular oscillations by just applying rather small controlling power.

Different strategies have been proposed how to achieve such a control:

(i) Modulation methods are either based on the synchronization to an external pe-

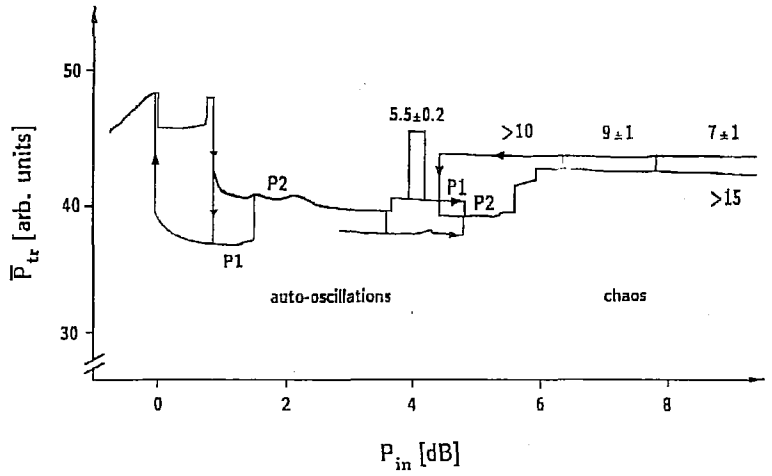

Fig. 9. Correlation dimensions estimated by the method of Grassberger and Procaccia (coincidence regime B, H=839 Oe). Two chaotic levels occur above 7 dB, differing in amplitude and dimension

riodic force with a frequency close to an intrinsic system frequency [43] or on the change of stability induced by a fast modulation of some system parameter [44]. A prominent example of the latter method is represented by the well-known Kapitza pendulum [45]. These simple non-feedback methods generally require rather large control power.

(ii) More sophisticated feedback control methods aim at the stabilization of existing, system inherent unstable periodic orbits. This can be achieved by a simple time-delayed feedback [46] or by calculated time-dependent corrections on one of the system parameters as proposed by OGY [30]. Since these techniques are making use of the intrinsic properties of the underlying chaotic attractor they can, in principle, be run with very small controlling power.

4.1. Method of OGY. The algorithm of OGY is based on the idea that chaotic attractors are generally embedded in an infinite number of unstable periodic orbits. If the trajectory comes into the vicinity of such a hyperbolic orbit, it approaches the orbit as long as the distance vector is located close to the *stable manifold*, and leaves it again in the direction of the *unstable manifold* (Fig.10). Since these processes evolve exponentially in time, they are rather slow in the vicinity of the orbit and can be affected by weak external perturbations. Unstable periodic orbits can be detected by means of the recurrence time method. In order to stabilise one of these orbits, one first has to calculate the evolution of a trajectory in its neighbourhood. Technically, this is achieved by reconstructing the trajectory (of e.g. a 3D flow) from a time series by means of time-delayed coordinates [41]. The problem is simplified by applying a Poincaré section perpendicular to the unstable periodic orbit, thus converting the 3D flow to a 2D discrete map (Fig.10). This way, the unstable periodic orbit is mapped to a hyperbolic fixed point $\xi_F(\mu_0)$ the stability of which has to be analysed. From the evolution of previous intersection points the stable and unstable eigenvalues λ_s and λ_u and the respective eigendirections $\mathbf{e}_s$ and $\mathbf{e}_u$ are determined. Such analysis yields a linearized prediction of the system dynamics in the neighbourhood of $\xi_F(\mu_0)$ where the evolution matrix can be expressed in terms of the stable and unstable eigenvalues ($\mathbf{e}_{s,u}$ and $\mathbf{e}_{s,u}^*$ denote the covariant and contravariant eigenvectors, respectively):

$$\xi_{n+1}(\mu_0) - \xi_F(\mu_0) \approx (\mathbf{e}_s\lambda_s\mathbf{e}_s^* + \mathbf{e}_u\lambda_u\mathbf{e}_u^*)[\xi_n(\mu_0) - \xi_F(\mu_0)]. \qquad (13)$$

Next, one considers a small change of the control parameter μ and calculates the corresponding shift $\mathbf{g}$ of this fixed point:

$$\mathbf{g} \equiv \partial\xi_F(\mu)/\partial\mu|_{\mu_0} \approx [\xi_F(\mu) - \xi_F(\mu_0)]/(\mu - \mu_0). \qquad (14)$$

The basic idea of OGY is to shift the fixed point and the corresponding evolution for a

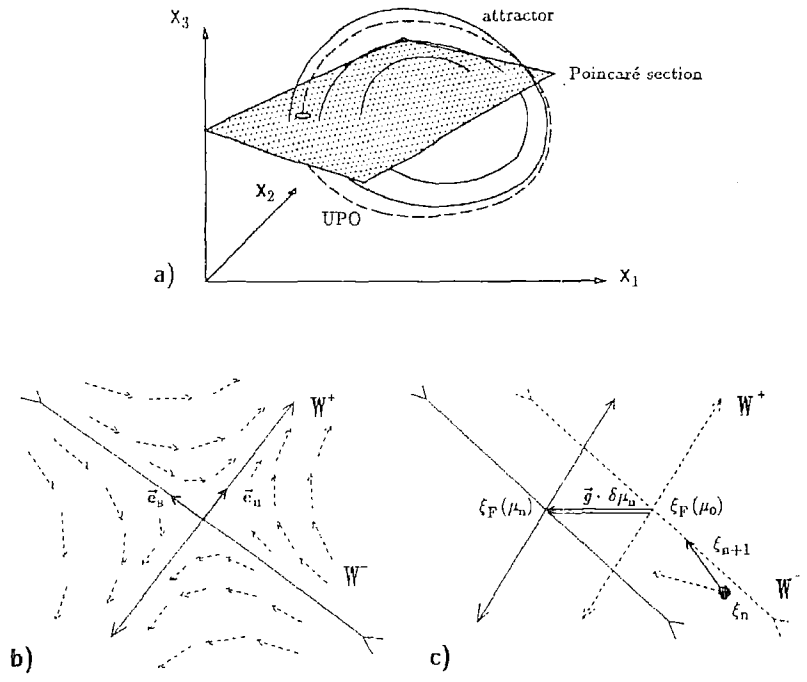

Fig. 10. Controlling scheme of OGY. a) Poincaré section and unstable periodic orbit. b) Neighbourhood of the fixed point ξ_F with stable and unstable manifolds W- and W+; dashed lines indicate shift of intersection points after one cycle. c) Effect of a small change of the control parameter μ (see text)

short time in such a way that after one cycle the system - described by $\xi_{n+1}(\mu \neq \mu_0)$ - ends up on the *stable manifold* of the original fixed point $\xi_F(\mu_0)$, and then to switch the perturbation off again. This way the following intersection points $\xi_{n+2}(\mu_0)$, $\xi_{n+3}(\mu_0)$,... exactly approach the fixed point without being repelled, i.e. after a well-targetted perturbation the intrinsic dynamics of the system is used for stabilizing the trajectory at the unstable periodic orbit. The value of this perturbation is obtained by combining eqs. (13), (14), and the condition that $\xi_{n+1}(\mu)$ be orthogonal to the unstable manifold:

$$\Delta\mu = \frac{\lambda_u}{\lambda_u - 1} \frac{(\xi_F(\mu_0) - \xi_F(\mu_0))\mathbf{e}_u^*}{\mathbf{g}\mathbf{e}_u^*} . \qquad (15)$$

Once the system has approached the orbit, the still necessary corrections (due to linearization error and noise) can be maintained by very small perturbations. Though originally developed for discrete maps, this concept can also be applied in low-dimensional continuous flows, but in practice is limited to only one unstable direction.

In contrast to our device Hunt is using a stroboscopic mapping for the Poincaré section and only one window, so his device is limited to non-autonomic, periodically driven systems.

4.2. Control by analog feedback device. Although the OGY method should apply to real experimental systems as well, in practice its application is restricted for the following reasons:

(i) Experimental systems often show high-dimensional chaos (*hyperchaos*), i.e. there is more than one unstable direction.

(ii) The measured signal is disturbed by noise; this may either prevent the control to work at all, if in the case of strong noise the system is pushed away from the neighbourhood of the fixed point, or at least reduces the sensitivity of the feedback in the case of weak noise.

(iii) The characteristic time scale of real systems can be too fast. For the magnetic

system investigated typical cycle times are in the order of μs (!), whereas the numerical calculation of the feedback signal requires at least some ms.

The first problem might be overcome by selecting only chaotic signals of sufficiently low dimensionality. Our Grassberger - Procaccia analyses showed that this is nearly impossible for the coincidence regime but rather easy to obtain in the case of non-resonant subsidiary absorption. Letter «C» in Fig.7 marks the corresponding range of control parameters where weak (*marginal*) chaos was observed. The chaotic signal to be controlled (Fig.12) was of the same type as analysed in Fig.8, which means characterized by D_2 =2.1±0.1, only one positive Lyapunov exponent λ_1=0.04(μs)$^{-1}$, and a mean cycle time of about 2 μs.

Since it was impossible to make numerical real-time predictions for a time scale of μs we had to modify the OGY algorithm in a way to be processed by an intelligent analog feedback device: For reconstructing the attractor we used analog time derivatives instead of time delay coordinates[3]. The Poincaré plane and the location of intersection points were determined by analog window discriminators for the signal and its first and second time derivatives triggering a track-and-hold amplifier (Fig.11a). The amplitude of the control signal was not determined from a preceding stability analysis of the periodic orbit. Instead, we used a feedback signal which is proportional to the deviation of the momentary signal $U(t_n)$ from the set-point (the «U-coordinate» of the phase space window to be adjusted to the position of the unstable orbit)

$$U_{contr}(t_n) = A[U(t_n) - U_{ref}] \qquad (16)$$

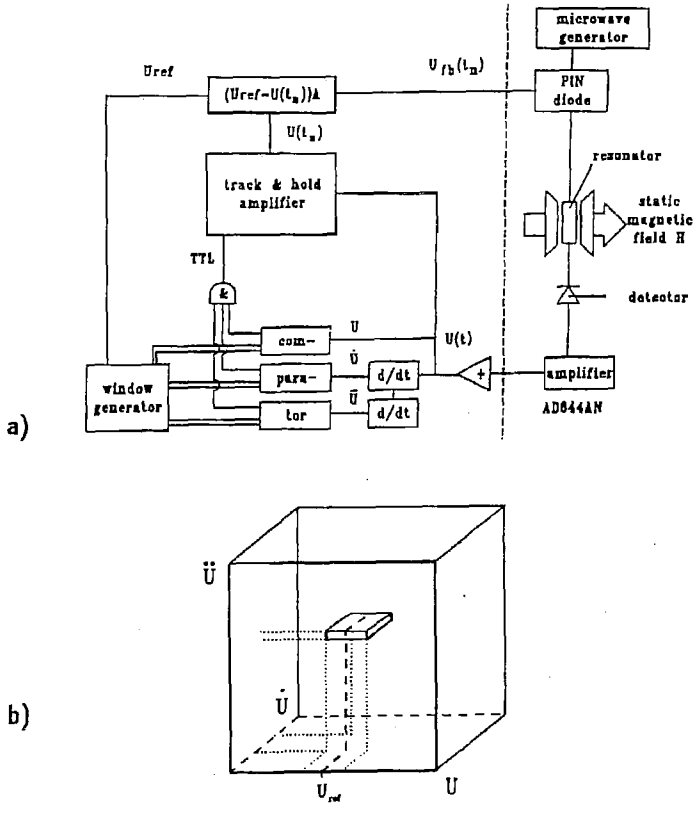

Fig. 11. Analog feedback device for controlling the chaotic FMR signal. a) Experimental set-up. b) Reconstruction of the phase space by means of analog derivatives. The small probe volume can be moved around by variating the settings of the window generator

[3] This choice of coordinates, in addition, avoids a possible instability of the controlling algorithm which may occur in the case of time-delay coordinates [47].

and variate the phase space coordinates in order to meet the neighbourhood of some unstable periodic orbit where the given feedback results in a proper control. A similar technique[4] was applied by Hunt [48] for controlling a diode-capacity resonator who called it *occasional proportional feedback*. There is complete correspondence of Eq.(16) to the original result of OGY, Eq.(15), identifying the amplification factor A with $\lambda_u(\lambda_u - 1)^{-1}(\mathbf{g}\mathbf{e}_u)^{-1}$ and the deviation $U(t_n) - U_{ref}$ with $(\xi_n(\mu) - \xi_F(\mu))\mathbf{e}_u$.

In our experiment the position of the unstable periodic orbit was selected by setting windows for the observed signal $U(t)$ and its first and second time derivative by means of analogy window comparators. The corresponding signal was held by an ultrafast track-and-hold amplifier. The deviation of this value from a given set-point is fed back to change the microwave pumping power. By careful adjustment of the windows and variation of the set-point we succeeded in suppressing the chaotic oscillations and stabilizing periodic orbits by means of a perturbation which is less than 10^{-3} of the actual pumping power P_{in}. The effect of control is illustrated by Fig. 12, where we have compared the chaotic signal before and after switching on the feedback. The controlled signal shows a very regular oscillation, and the corresponding phase space trajectory, in fact, consists of a single orbit slightly smeared out by noise. To our knowledge this is the first and fastest

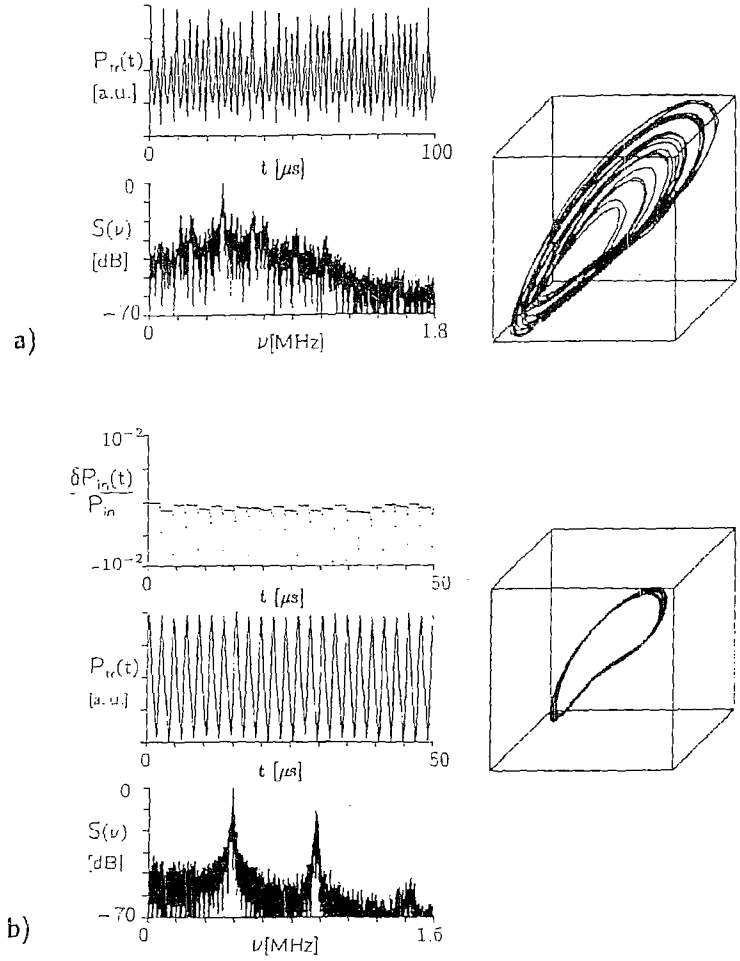

Fig. 12. Result of the feedback control. a) Chaotic time signal, spectrum and reconstructed attractor without control. b) Control signal, regular oscillations, spectrum and stabilized orbit after having switched on the control

[4] In contrast to our device Hunt is using a stroboscopic mapping for the Poincaré section and only one window, so his device is limited to non-autonom, periodically driven systems.

experimental control of chaos in spin-wave turbulence using a feedback system which stabilizes the inherent periodic dynamics of a strange attractor.

5. Conclusions

The experimental results presented in this article indicate that transverse-pumped YIG spheres at the first-order Suhl instability are of particular interest for studying concepts of nonlinear dynamics in real solids. The experimental conditions differ from the more often investigated second-order Suhl instability or from parallel pumping by the variety and complexity of the observed phenomena, and also by more complicated nonlinear mechanisms. Most of the effects reported in previous investigations, such as period doublings, quasiperiodicity, or mode-locking, have been observed in this system, but also new phenomena were found: sudden jumps in the transmitted FMR signal and a well reproducible multistability. We have tried to classify the observed bifurcation scenarios, to characterize the chaotic state, and to draw physical conclusions from this information. For a quantitative theoretical interpretation of these phenomena based on three-magnon processes and a novel indirect coupling mechanism via degenerate modes, which was found to be much stronger in the coincidence regime than conventional four-magnon processes, we refer to the literature [26-29]. Finally, as a first possible application of nonlinear dynamics, we have considered the problem of chaos suppression effected by very weak external forces. By means of an analog feedback device related to the controlling scheme of Ott, Grebogi, and Yorke we succeeded in stabilizing inherent unstable periodic orbits with the help of very weak external time-dependent perturbations.

Altogether, we have seen that the investigation of spin systems represents a very interesting topic both from the viewpoint of solid-state physics and of nonlinear dynamics. The reasons are manifold:

(i) They represent intrinsically nonlinear systems with nonlinearities originating from well-known interactions.

(ii) Their nonlinearities can partly be controlled by external fields - as in the present example.

(iii) Their nonlocal couplings allow the formation of spatio-temporal patterns. Nevertheless, in experiment one meets the problem that most of the interesting phenomena in spin systems occur on rather inconvenient time and length scales. While the time scale of auto-oscillations - typically one microsecond - remains accessible by modern electronics, it has been impossible so far to resolve dynamic magnetic patterns of micrometer size. Conventional magnetic resonance only probes the uniform mode, optical scattering experiments, in general, suffer from too low resolution. Very recently, new techniques for recording the local magnetization have been developed [49,50]. If they could be improved to probe standing spin waves, then again the coincidence regime would offer favourite conditions, because of the long-wavelength modes involved. Such investigations could be of crucial importance for confirming or modifying our present understanding of the underlying nonlinear mechanisms.

Acknowledgements

We thank Prof.Dr.W.Tolksdorf from Philips Research Laboratory, Hamburg, for supplying us with high quality samples. This project of SFB 185 «Nichtlineare Dynamik» was partly financed by special funds of the Deutsche Forschungsgemeinschaft.

References

1. *R.W. Damon* in: Magnetism, Vol. 1, ed. by G.T. Rado and H. Suhl (Academic, New York 1963) pp. 551.
2. *R.W. Damon*: Rev. Mod. Phys. **25**, 239 (1953).
3. *N. Bloembergen, S. Wang*: Phys. Rev. **93**, 72 (1954).
4. *F.R. Morgenthaler*: J. Appl. Phys. **31**, 95S (1960).
5. *E.S. Schlömann, J.J. Green, U. Milano*: J. Appl. Phys. **31**, 386S (1960).
6. *H. Suhl*: J. Phys. Chem. Solids **1**, 209 (1957).
7. *V.E. Zakharov, V.S. L'vov, S.S. Starobinets*: Sov. Phys. Usp. **17**, 896 (1975).

8. *V.S. L'vov, L.A. Prozorova* in: Spin Waves and Magnetic Excitations, Vol. 1, ed. by A.S. Borovik-Romanov and S.K. Sinha (Elsevier, Amsterdam 1988) pp. 233-285.
9. Nonlinear Phenomena and Chaos in Magnetic Materials ed. Ph. E. Wigen (World Scientific, Singapore, New Jersey 1994).
10. *G. Gibson, C. Jeffries*: Phys. Rev. A **29**, 811 (1984).
11. *F. Waldner, D.R. Barberis, H. Yamazaki*: Phys. Rev. A **31**, 420 (1985); H. Yamazaki, M. Warden: J. Phys. Soc. Jpn. **55**, 4477 (1986).
12. *F.M. de Aguiar, S.M. Rezende*: Phys. Rev. Lett. **56**, 1070 (1986); *F.M. de Aguiar, A. Azevedo, S.M. Rezende*: Phys. Rev. B **39**, 9448 (1989).
13. *T.L. Caroll, L.M. Pecora, F.J. Rachford*: J. Appl. Phys. **64**, 5396 (1988) ; Phys. Rev. A **42**, 377 (1989).
14. *H. Benner, F. Rödelsperger, H. Seitz, G. Wiese*: J. de Physique, Colloque C8, **49**, 1603 (1988); *H. Benner, F. Rödelsperger, G. Wiese,* in: Nonlinear Dynamics in Solids, ed. H.Thomas (Springer, Berlin, Heidelberg 1992).
15. *M. Warden, F. Waldner*: J. Appl. Phys. **64**, 5386 (1988).
16. *P. E. Wigen, H. Dötsch, M. Ye, L. Baselgia, F. Waldner:* J. Appl. Phys. **63**, 4157 (1988).
17. *P.H. Bryant, C.D. Jeffries, K. Nakamura*: Phys. Rev. A **38**, 4223 (1988).
18. *H. Yamazaki, M. Mino*: Progr. Theor. Phys. Suppl. **98**, 400 (1989).
19. *K. Nakamura, S. Ohta, K. Kawasaki*: J. Phys. C **15**, L 143 (1982).
20. *X.Y. Zhang, H. Suhl*: Phys. Rev. A **32**, 2530 (1985).
21. *S.M. Rezende, O.F. de Alcantara Bonfim, F.M. de Aguiar*: Phys. Rev. B **33**, 5153 (1986).
22. *X.Y. Zhang, H. Suhl*: Phys. Rev. B **38**, 4893 (1988).
23. *S.P. Lim, D.L. Huber*: Phys. Rev. B **37**, 5426 (1988).
24. *V.B. Cherepanov, A.N. Slavin*: Phys. Rev. B **47**, 5874 (1993).
25. *F. Waldner:* J. Phys. C **21**, 1243 (1988).
26. *G. Wiese, H. Benner*: Z. Phys. B **79**, 119 (1990).
27. *G. Wiese, H.-A. Krug von Nidda, H. Benner*: Europhys. Lett. **15**, 585 (1991).
28. *G. Wiese:* Z. Phys. B **82**, 453 (1991).
29. *H.-A. Krug von Nidda, G. Wiese, H. Benner:* Z. Phys. B **95**, 55 (1994).
30. *E. Ott, C. Grebogi and J.A Yorke*: Phys. Rev. Lett. **64**, 1196 (1990).
31. *Landolt-Börnstein*: New Series, Vol. III/4a (Springer, Berlin, Heidelberg 1970) p. 315.
32. see e.g. *H.G. Schuster*: Deterministic Chaos (2. rev. ed.) (VCH, Weinheim 1988).
33. *F. Rödelsperger*, Chaos und Spinwelleninstabilitäten (Harri Deutsch, Frankfurt 1994); *F. Rödelsperger, H. Benner, A. Cenys,* to be published.
34. *Y. Pomeau, P. Manneville*: Commun. Math. Phys. **74**, 189 (1980).
35. *F.M. de Aguiar*: Phys. Rev. A **40**, 7244 (1989).
36. *F. Rödelsperger, T. Weyrauch, H. Benner*: J. Magn. Magn. Mater. (1992).
37. *C. Grebogi, E. Ott, J.A. Yorke*: Physica **7**D, 181 (1983); *C. Grebogi, E. Ott, F. Romeiras, J.A. Yorke*: Phys. Rev. A **36**, 5365 (1987).
38. *C.E. Patton, W. Jantz*: J. Appl. Phys. 50, 7082 (1979); *M. Chen, C.E. Patton*: J. Appl, Phys. **69**, 5724 (1991).
39. *P. Bergé, Y.Pomeau, C.Vidal*: Order within Chaos (Wiley, NewYork 1986) pp. 247-258.
40. *Y.B. Pesin:* Usp. Mat. Nauk **32**, 55 (1977).
41. *F. Takens* in: Lecture Notes in Mathematics, ed. by D. A. Rand and L.S. Young (Springer, Berlin, Heidelberg 1981) Vol. 898, p. 366.
42. *P. Grassberger, I. Procaccia*: Physica **9**D, 189 (1983); Phys. Rev. A **28**, 2591 (1983).
43. *V.V. Alekseev, A.Yu. Loskutov*: Dokl. Akad. Nauk SSSR **293**, 1346 (1987); *R. Lima, M. Pettini*: Phys. Rev. A **41** (1990) 726 ; ibid. **47**, 4630 (1993).
44. *S. Parthasarathy*: Phys. Rev. A **46**, 2147 (1992); *Y.S.Kivshar, F. Rödelsperger, H. Benner*: Phys. Rev. E **49** (1994) 319.
45. *L.D. Landau, M. Lifshitz*, Mechanics (Pergamon Press, Oxford, 1960).
46. *K. Pyragas*: Phys. Lett. A **170** (1992) 421.
47. *U. Dressler, G. Nitsche*: Phys. Rev. Lett. **68**, 1 (1992).
48. *E.R. Hunt*, Phys. Rev. Lett. **67**, 1953 (1991).
49. *D. Rugar, H.J. Mamin, R. Erlandson, J.E. Stern, B.D. Terris*: IBM Research Report RJ 6272 (1988).
50. *J. Pelzl, B.K. Bein*: Phys. Bl. 46, 12 (1990); *F. Rödelsperger, O. von Geisau, H. Benner, J. Pelzl*: Proc. XXVI Congress Ampère on Magnetic Resonance, Athens 1992, p. 116.

Institut für Festkörperphysik,
Technische Hochschule Darmstadt,
Federal Republic of Germany

Поступила в редакцию 14.01.95 г.

АНАЛИЗ И НАБЛЮДЕНИЕ ХАОСА
ПРИ СПИН-ВОЛНОВОЙ НЕСТАБИЛЬНОСТИ

Г. Беннер, Р. Хенн, Ф. Рёделыпергер, Г. Визе

Ферромагнитные образцы, возбуждаемые сильным высокочастотным полем, демонстрируют разнообразные нелинейные явления. Описываются эксперименты по ферромагнитному резонансу в образцах жёлезо-иттриевого граната (ЖИГ) обнаруживающие спин-волновую нестабильность при сигналах выше порогового уровня первого порядка по Сулу. Выявлено и проанализировано множество различных сценариев, а именно: удвоение периода, квазипериодичность, различные типы перемежаемости совместно с очень сложными явлениями мультистабильности. В случае нерезонансного возбуждения однородной моды исследуемые хаотические колебания относятся к низко-размерному аттрактору (D_2≈2.1) с характерным временным масштабом порядка μs, в то время как для резонансного возбуждения получаются очень высокоразмерные аттракторы (D_2≈7 … >15). Для стабилизации неустойчивых циклов в такой быстрой системы разработано устройство с обратной связью, относящееся к управляющей схеме Ott, Grebogi и Yorke. Подавление низко-размерного хаоса осуществлялось введением малого (зависимого от времени) сигнала обратной связи порядка 10^{-3} амплитуды входного высокочастотного поля.

Benner Hartmut - born in 1945. Diploma in Physics at Technische Hochschule Darmstadt (THD), Scholarship of *Studienstiftung des deutschen Volkes* (1973). Ph.D. thesis on non-Markovian dynamics in magnetic low dimensional systems (1979). Visiting Scientist at Centre d'Etude Nucleaires de Grenoble, France (1981). Habilitation on nonlinear spin dynamics in magnetic insulators (1988). Head of the experimental Nonlinear Spin Dynamics Group at the Institute of Solid State Physics, THD, probing nonlinear phenomena in magnetic systems by means of resonance techniques (NMR, FMR. AFMR). Scientific interests: High temperature and critical dynamics of low-dimensional Heisenberg magnets; Topological solitons in ferro- and antiferromagnetic spin chains; Spin-wave turbulence; Parametric excitation of nuclear spin waves and magneto-elastic waves; Theory of solitons and chaos; Analysis of time series data; Chaos control; Stochastic resonance; Pattern formation in magnetic films. More than 60 publications.

Henn Rüdiger - born in 1965. Diploma in Physics at Technische Hochschule Darmstadt, Thesis on chaos control in fast experimental systems (1993). Now at Max Planck Institute for Solid State Research, Stuttgart, preparing a Ph.D. thesis on superconductivity in low-dimensional metals.

Rödelsperger Frank - born in 1963. Diploma in Physics at Technische Hochschule Darmstadt, Thesis on experimental and theoretical analysis of time series data (1989). Ph.D. thesis on concepts of nonlinear dynamics in spin-wave instabilities (1994). Scientific interests: Spin-wave instabilities and chaos observed by high-power FMR; Theory of chaos; Analysis of time series data; Chaos control in spin systems. About 15 publications, author of a book on Spin-wave instabilities and Chaos. Now chief efficiency expert at Gaggenau Industries, Germany.

Wiese Garrelt - born in 1962. Diploma in Physics at Technische Hochschule Darmstadt (THD), Thesis in experimental solid state physics (1986). Ph.D. thesis on instabilities and chaos in high-power ferromagnetic resonance experiments (1991). Visiting Scientist at the Department of Physics of Colorado State University (1992). Scientist at the Institute of Solid State Physics, THD, Scholarship of German Research Foundation (DFG) (1993). Scientific interests: Microwave and light scattering spectroscopy; Spin-wave instabilities and chaos observed by high-power FMR; Theory of parametric excitation of spin waves in ferromagnetic spheres and films; Analysis of chaos. More than 20 publications. Now project manager at Telekom, Germany.